Hyperentanglement source by intersubband two-photon emission from semiconductor quantum wells

Alex Hayat,* Pavel Ginzburg, David Neiman, Serge Rosenblum, and Meir Orenstein

Department of Electrical Engineering, Technion, Haifa 32000, Israel
**Corresponding author: ahayat@tx.technion.ac.il*

Received December 6, 2007; revised April 15, 2008; accepted April 17, 2008;
posted April 21, 2008 (Doc. ID 90619); published May 22, 2008

We propose an efficient hyperentanglement source emitting photon pairs entangled in both energy and polarization. The compact electrically driven room-temperature source, based on intersubband two-photon emission from semiconductor quantum wells (QWs) exhibits pair generation rates several orders of magnitude higher than alternative conventional schemes. A theoretical formalism is derived for the calculation of photon pair generation spectra and rates. The results are presented for superlattice structures similar to quantum cascade lasers of GaAs/AlGaAs QWs emitting in the mid-IR and far-IR and for InN/AlN QW structures suitable for telecommunication wavelengths. © 2008 Optical Society of America

OCIS codes: 270.4180, 270.5565.

Various applications of quantum information processing require efficient and reliable sources of entangled photons [1–3]. Entanglement in more than one degree of freedom (hyperentanglement) [4] was shown to provide higher quality quantum information processing [5]. Moreover, using high-dimensional entanglement significantly improves quantum data security [6] and quantum metrology [7]. Currently, the most widely used approach to generate hyperentangled photon pairs is based on spontaneous parametric downconversion (PDC) [8]. A substantial research effort has been made to miniaturize and enhance PDC [9,10], limited, however, by the relatively weak $\chi^{(2)}$ interaction. Moreover, PDC requires dispersion compensation techniques using material birefringence or quasi-phase matching [11] as well as strong optical pumping. A promising technique was demonstrated for the generation of photon pairs via fiber Kerr nonlinearity [12–15], where photons are inherently coupled into the fiber spatial modes with the small $\chi^{(3)}$ nonlinearity being the limiting factor. Quantum dot devices offer an alternative means of creating entangled photons [16,17]. However, their cryogenic operation and low emission rates prevent the integration of these sources into communication systems. Recently, a compact current-driven entanglement source was proposed based on interband two-photon emission (TPE) from a semiconductor device [18,19] offering much higher pair generation rates and technological feasibility.

Here we propose a compact high-intensity source of hyperentangled photons based on intersubband TPE in electrically pumped semiconductor quantum wells (QWs) at room temperature that does not require any phase matching. In TPE, a photon pair is simultaneously emitted by a single electron undergoing a level transition. We analyze semiconductor QW intersubband TPE processes in contrast to the previously considered interband TPE [18]. In some QW intersubband TPE transitions, the in-plane emitted photons are orthogonally polarized owing to the selection rules [20,21], which do not determine, however, the polarization of each individual photon. Furthermore, the energies of the two emitted photons must sum up to the electronic energy difference owing to energy conservation, while each photon's energy is not determined. Therefore the photon pairs will be hyperentangled in both energy [22] and polarization. The implementation of such devices is feasible using configurations similar to those of quantum cascade lasers (QCLs). The TPE probability is calculated using the $H_{\mathrm{int}}=-e/m_0\hat{\mathbf{p}}\cdot\hat{\mathbf{A}}$ Hamiltonian, where $\hat{\mathbf{A}}$ and $\hat{\mathbf{p}}$ are the vector potential and electron momentum operators, respectively. The transition amplitude is given by the second order time-dependent perturbation theory [23]:

$$S=\frac{k_e e^2}{m_0^2 n_r^2\sqrt{\omega_1\omega_2}}\frac{2\pi\hbar}{V}\sum_{\nu}\left\{\frac{\langle\psi_f|\mathbf{p}\cdot\varepsilon_2|\psi_\nu\rangle\langle\psi_\nu|\mathbf{p}\cdot\varepsilon_1|\psi_i\rangle}{\hbar\omega_1+E_\nu+i\Gamma-E_i}+\frac{\langle\psi_f|\mathbf{p}\cdot\varepsilon_1|\psi_\nu\rangle\langle\psi_\nu|\mathbf{p}\cdot\varepsilon_2|\psi_i\rangle}{\hbar\omega_2+E_\nu+i\Gamma-E_i}\right\},\tag{1}$$

where $|\psi_i\rangle$ and $|\psi_f\rangle$ are the initial and final electron states, $|\psi_\nu\rangle$ are the intermediate states that span the virtual state, e and m_0 are the free electron charge and mass, $k_e=1/4\pi\varepsilon_0$, $\varepsilon_{1,2}$ are the photon polarizations, $\omega_{1,2}$ are the photon frequencies, V is the quantization volume, Γ is the dephasing, and n_r is the material's refractive index. QW electron wave functions can be written as

$$|\psi_n\rangle=e^{ik_x x+ik_y y}\phi_n(z)u_{\mathbf{k}}(\mathbf{r}),\tag{2}$$

where $u_{\mathbf{k}}(\mathbf{r})$ is the crystal's Bloch function, k_x and k_y are the two orthogonal in-plane crystal momentum components, and $\phi_n(z)$ is the envelope function in the layer growth direction z. Assuming that $\phi_n(z)$ varies slowly over a crystal unit cell, the matrix elements are [24,25]

$$\langle \psi_f | \varepsilon \cdot \mathbf{p} | \psi_i \rangle = \begin{cases} \hbar(m_0/m_i)\varepsilon_\perp \cdot \mathbf{k}_{e,\perp} & \Delta n = 0 \\ \varepsilon_z p_{if} & \Delta n \text{ odd} \\ 0 & \Delta n \neq 0, \text{ even}, \end{cases} \tag{3}$$

where $p_{if}=\int \phi_f(z) p_z \phi_i(z) \mathrm{d}z$; Δn is the transition subband index difference; $\varepsilon_\perp$ and $\mathbf{k}_{e,\perp}$ are the in-plane photon polarization vector and in-plane electron crystal momentum, respectively; and m_n is the effective electron mass in the nth conduction subband.

In a two-level QW the only contributing intermediate states are the initial and the final states [21] yielding orthogonal photon polarizations [Eq. (3)], one z polarized photon and one in-plane polarized photon (Fig. 1). Moreover, the emitted photon energies are complementary but not individually defined. Hence, for the in-plane emitted pairs the general hyperentangled state is

$$\psi = \int g(\omega)[|\omega, \varepsilon_z\rangle_1 |\omega_{if} - \omega, \varepsilon_\perp\rangle_2 + |\omega, \varepsilon_\perp\rangle_1 |\omega_{if} - \omega, \varepsilon_z\rangle_2] \mathrm{d}\omega, \tag{4}$$

where $|g(\omega)|^2$ is the normalized emitted spectral density per given carrier energy. The pair emission rate is given by

$$W = \int R_{sp} \rho_e(\mathbf{k}_{e,\perp}) \rho_{\mathrm{ph}}(\mathbf{k}_1) \rho_{\mathrm{ph}}(\mathbf{k}_2) f_i(1-f_f) \mathrm{d}^3k_1 \mathrm{d}^3k_2 \mathrm{d}^2k_e, \tag{5}$$

where $\rho_e(\mathbf{k}_{e,\perp})$ is the electronic reduced density of states, $\rho_{\mathrm{ph}}(\mathbf{k}_i)$ is the photonic state density with $\mathbf{k}_i$ (the photon wavenumber), f_n is the Fermi–Dirac distribution of the nth subband, and R_{sp} is the emission rate for the given final and initial states. In the case of intersubband transitions,

$$\rho_e(\mathbf{k}_{e,\perp}) f_i(1-f_f) = \frac{1}{2\pi^2}[1 + e^{\beta(E(k_\perp)-E_{F,i})}]^{-1} \times [1 + e^{\beta(E_{F,f}-E(k_\perp))}]^{-1}, \tag{6}$$

where $E(k_\perp)$ represents the initial in-plane kinetic energy of the electron and $E_{F,n}$ denotes the quasi-Fermi level of the nth subband that for a two-dimensional electron gas is [26]

$$E_{F,n} = \beta^{-1} \ln\left[\exp\left(\beta \frac{\pi\hbar^2}{m} N_n\right) - 1\right], \tag{7}$$

with N_n as the electron sheet density and $\beta = 1/(k_b T)$, where k_b is the Boltzmann constant and T is the temperature. The rate of emission per frequency is

$$\frac{\partial W}{\partial \omega} = B\omega(\omega_{if} - \omega) \left| \frac{k_e e^2 m_i n_r p_{if}}{\pi\hbar^2 m_0^2 \beta c^3} \right|^2 \left| \frac{(1+m_0/m_i)}{(\omega + i\Gamma/\hbar)} + \frac{(1+m_0/m_f)}{(\omega - \omega_{if} + i\Gamma/\hbar)} - \frac{(1+m_0/m_i)}{(\omega - \omega_{if} - i\Gamma/\hbar)} - \frac{(1+m_0/m_f)}{(\omega - i\Gamma/\hbar)} \right|^2, \tag{8}$$

where $B = \int_0^\infty x[1+e^{(x-\beta E_{F,i})}]^{-1}[1+e^{(\beta E_{F,f}-x)}]^{-1}\mathrm{d}x$.

As an example of a mature-technology 1000 QW superlattice [27], the pair generation rate was calculated for 7 nm thick GaAs/$Al_{0.2}Ga_{0.8}$As QWs (Fig. 2); m_n was approximated by $m_n^{-1} = P_n m_{\mathrm{in}}^{-1} + (1-P_n) m_{\mathrm{out}}^{-1}$, where P_n is the nth level confinement factor and m_{in} and m_{out} are the QW and barrier effective masses, respectively [28]. The electron lifetime in the ground state is assumed to be much shorter than that of the excited state owing to efficient draining mechanisms [29,30]. The transition dephasing, mostly determined by the carrier decoherence time, is assumed to be less than 100 fs.

According to the calculations for injection currents corresponding to carrier sheet densities of about $10^{12}\,\mathrm{cm}^{-2}$ and assuming a $100\,\mu\mathrm{m}^2$ device, the GaAs/$Al_{0.2}Ga_{0.8}$As QW pair generation rates are about 1 KHz/mW/nm. This efficiency is slightly below the best reported fiber-optical (~50 KHz/mW/nm) [15] and PDC-based rates [31]. However, using doubly resonant microcavities, the TPE spectrum can be concentrated into two narrow wavelength windows [18], thus increasing the per-wavelength emission rates by several orders of magnitude.

The main limitation of employing intersubband GaAs devices is the long mid-IR to far-IR range,

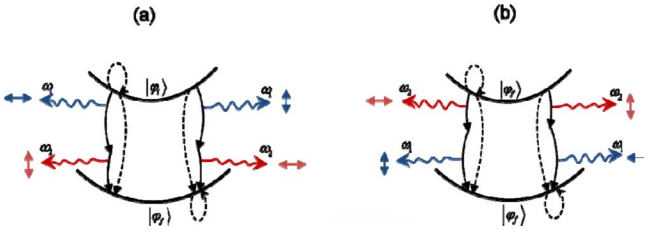

Fig. 1. (Color online) Schematic of a QW intersubband TPE with orthogonal polarizations. The solid arrows are the electronic transitions via virtual states while the dashed arrows represent the matrix element calculations via intermediate states. (a) and (b) Symmetrical Feynman diagrams with interchanged vertices.

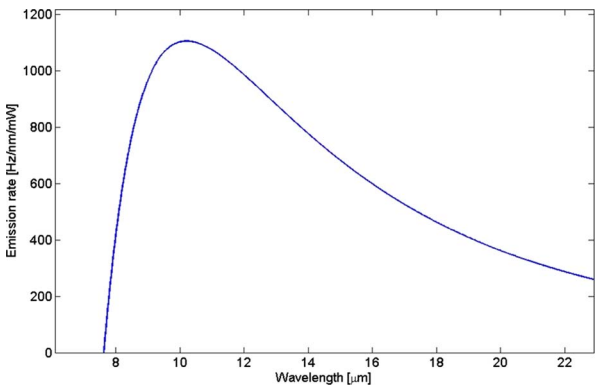

Fig. 2. (Color online) TPE rate per nanometer wavelength per milliwatt input power for a GaAs/$Al_{0.2}Ga_{0.8}$As superlattice with a $100\,\mu\mathrm{m}^2$ device area and a 7 nm QW thickness.

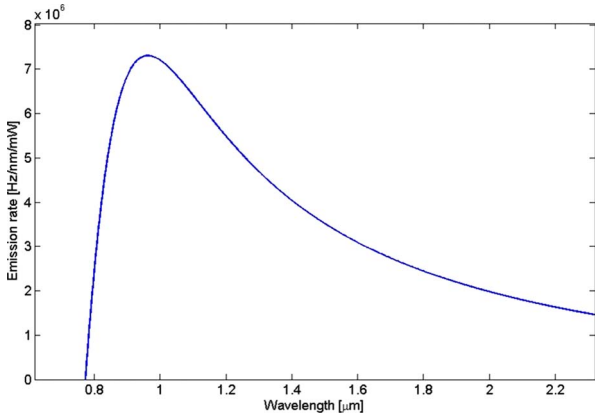

Fig. 3. (Color online) TPE rate per nanometer wavelength per milliwatt input power for an InN/AlN superlattice with a 100 μm^2 device area and a 1.3 nm QW thickness.

which requires cooling to ~60 K to achieve TPE, which is an order of magnitude stronger than blackbody radiation. Owing to the lack of optical pumping in the proposed scheme, no parasitic optical nonlinearities affect the performance.

A potential semiconductor device for room-temperature telecom-wavelength hyperentanglement generation may be based on nitride-compound QWs, for example, InN/AlN QWs [32]. For a 1.3 nm InN/AlN QW, the calculated pair emission spectrum is centered at the near-IR wavelength (Fig. 3). For a ~100 μm^2 device the rates are 10^4 KHz/mW/nm, 3 orders of magnitude higher than the alternative reported photon pair sources. In the proposed near-IR device the blackbody radiation is 8 orders of magnitude weaker than TPE at room temperature and can be neglected. There is a trade-off between the high emission rates and the achievable fidelity. We estimated the multiple pair emission probability per temporal mode to be less than 1% for an ~10% single pair generation per temporal mode, which is comparable to the reported PDC-based sources [33].

In conclusion, we have theoretically demonstrated an electrically driven room-temperature hyperentanglement source emitting photon pairs entangled in energy and polarization. Such devices emitting in the mid-IR and far-IR can be implemented using existing QCL technologies. In addition, potential devices in the telecom-wavelength range can be realized using nitride-based materials [34], allowing for their integration into the existing fiber-optic communication infrastructure. These TPE-based entanglement sources exhibit pair generation rates several orders of magnitude higher than the alternative schemes. Much simpler design and fabrication considerations make them promising candidates for future real-world quantum information technologies as well as for quantum metrology.

References

1. P. Kumar, P. Kwiat, A. Migdall, S. Nam, J. Vuckovic, and F. N. C. Wong, Quantum Inf. Process. **3**, 215 (2004).
2. J. S. Bell, Physics (Long Island City, N.Y.) **1**, 195 (1964).
3. T. B. Pittman and J. D. Franson, Phys. Rev. Lett. **90**, 240401 (2003).
4. T.-C. Wei, J. T. Barreiro, and P. G. Kwiat, Phys. Rev. A **75**, 060305(R) (2007).
5. S. P. Walborn, S. Pádua, and C. H. Monken, Phys. Rev. A **68**, 042313 (2003).
6. N. K. Langford, T. J. Weinhold, R. Prevedel, A. Gilchrist, J. L. O'Brien, G. J. Pryde, and A. G. White, Phys. Rev. Lett. **95**, 210504 (2005).
7. M. W. Mitchell, J. S. Lundeen, and A. M. Steinberg, Nature **429**, 161 (2004).
8. A. B. U'Ren, R. K. Erdmann, M. de la Cruz-Gutierrez, and I. A. Walmsley, Phys. Rev. Lett. **97**, 223602 (2006).
9. L. Lanco, S. Ducci, J. P. Likforman, X. Marcadet, J. A. W. van Houwelingen, H. Zbinden, G. Leo, and V. Berger, Phys. Rev. Lett. **97**, 173901 (2006).
10. G. Klemens, C.-H. Chen, and Y. Fainman, Opt. Express **13**, 9388 (2005).
11. K. Banaszek, A. B. U'Ren, and I. A. Walmsley, Opt. Lett. **26**, 1367 (2001).
12. X. Li, P. L. Voss, J. E. Sharping, and P. Kumar, Phys. Rev. Lett. **94**, 053601 (2005).
13. J. Fan and A. Migdall, Opt. Express **15**, 2915 (2007).
14. C. Liang, K. F. Lee, M. Medic, P. Kumar, R. H. Hadfield, and S. W. Nam, Opt. Express **15**, 1322 (2007).
15. J. Fan, A. Migdall, and L. J. Wang, Opt. Lett. **30**, 3368 (2005).
16. N. Akopian, N. H. Linder, E. Poem, Y. Berlatzky, J. Avron, D. Gershoni, B. D. Geradot, and P. M. Petroff, Phys. Rev. Lett. **96**, 130501 (2006).
17. R. M. Stevenson, R. J. Young, P. Atkinson, K. Cooper, D. A. Ritchie, and A. J. Shields, Nature **439**, 179 (2006).
18. A. Hayat, P. Ginzburg, and M. Orenstein, Phys. Rev. B **76**, 035339 (2007).
19. A. Hayat, P. Ginzburg, and M. Orenstein, Nat. Photonics **2**, 238 (2008).
20. E. Rosencher, J. Appl. Phys. **73**, 1909 (1993).
21. H. C. Liu, M. Buchanan, and Z. R. Wasilewski, Appl. Phys. Lett. **72**, 1682 (1998).
22. J. D. Franson, Phys. Rev. Lett. **62**, 2205 (1989).
23. N. G. Basov, A. Z. Grasiuk, V. F. Efimov, I. G. Zubarev, V. A. Katulin, and Ju. M. Popov, J. Phys. Soc. Jpn. **21**, 277 (1966).
24. C. C. Lee and H. Y. Fan, Phys. Rev. B **9**, 3502 (1974).
25. E. West, Appl. Phys. Lett. **46**, 1156 (1985).
26. S. L. Chuang, *Physics of Optoelectronic Devices* (Wiley-Interscience, 1995).
27. S. Pascarelli, F. Boscherini, C. Lamberti, and S. Mobilio, Phys. Rev. B **56**, 1936 (1997).
28. M. E. Levinshtein, S. L. Rumyantsev, and M. Shur, eds., *Handbook Series on Semiconductor Parameters* (World Scientific, 1996).
29. J. Faist, F. Capasso, D. L. Sivco, C. Sirtori, A. L. Hutchinson, and A. Y. Cho, Science **264**, 553 (1994).
30. D. A. Carder, L. R. Wilson, R. P. Green, J. W. Cockburn, M. Hopkinson, M. J. Steer, R. Airey, and G. Hill, Appl. Phys. Lett. **82**, 3409 (2003).
31. M. Pelton, P. Marsden, D. Ljunggren, M. Tengner, A. Karlsson, A. Fragemann, C. Canalias, and F. Laurell, Opt. Express **12**, 3573 (2004).
32. B. Monemar and G. Pozina, Prog. Quantum Electron. **24**, 239 (2000).
33. O. Kuzucu and F. N. C. Wong, Phys. Rev. A **77**, 032314 (2008).
34. E. Berkowicz, D. Gershoni, G. Bahir, A. C. Abare, S. P. DenBaars, and L. A. Coldren, Phys. Status Solidi B **216**, 291 (1999).